Vol 16 No 5, May 2007
1009-1963/2007/16(05)/1391-08
Chinese Physics
© 2007 Chin. Phys. Soc.
and IOP Publishing Ltd

Diffusion-induced deflection and the effect of two-wave mixing gain on dissipative photovoltaic solitons*

Liu Shi-Xiong(刘时雄)†, Liu Jin-Song(刘劲松)‡, Zhang Hui-Lan(张绘蓝), Zhang Guang-Yong(张光勇), and Wang Cheng(王 程)

School of Optoelectronics Science and Engineering, State Key Laboratory of Laser Technology, Huazhong University of Science and Technology, Wuhan 430074, *China*

(Received 25 June 2006; revised manuscript received 18 December 2006)

In an open-circuit dissipative photovoltaic (PV) crystal, by considering the diffusion effect, the deflection of bright dissipative photovoltaic (DPV) solitons has been investigated by employing numerical technique and perturbational procedure. The relevant results show that the centre of the optical beam moves along a parabolic trajectory, while the central spatial-frequency component shifts linearly with the propagation distance; furthermore, both the spatial deflection and the angular derivation are associated with the photovoltaic field. Such DPV solitons have a fixed deflection degree completely determined by the parameters of the dissipative system. The small bending cannot affect the formation of the DPV soliton via two-wave mixing.

Keywords: deflection, dissipative photovoltaic soliton, two-wave mixing
PACC: 4265J, 7240, 4240E

1. Introduction

It has been known that photorefractive (PR) crystals can be used to form and support optical solitons[1,2] which have been widely investigated in theory and experiment,[3−17] such as photovoltaic solitons,[14−20] screening solitons[5,6] and screening-photovoltaic (SP) solitons.[7,8] In 2002, Cohen *et al* proposed a kind of holographic soliton (HS)[21] especially the HS in a dissipative system.[22,23] We can obtain a thorough review of recent work on spatial optical solitons in PR crystals by consulting Ref.[24].

In 2003, the rigid photovoltaic (RPV) soliton was proposed,[23] and such solitons were assumed to occur in a nonlinearly amplifying or absorbing system consisting of a photovoltaic crystal and a strong pump beam with a uniform spatial distribution in both transverse dimensions. The self-trapping beam (also called signal beam) in the dissipative system can evolve into a spatial soliton when it couples coherently with the pump beam by two-wave mixing (TWM). The signal and pump beams are governed by a coupled-wave equation (CWE). Although the evolutions of the pump and signal beams should be described by the CWE, under an undepleted pump approximation and by ignoring the effect of self-focusing nonlinearity on the pump beam (namely under the small-signal condition), the CWE can be simplified into an evolution equation for the signal beam alone. In what follows, we refer to the evolution equation as small-signal equation (SSE). The bright and dark analytical solitary solutions for the signal beam are obtained from the SSE when the diffusion effect is not considered.[23] Because the system supporting such solitons is a dissipative one, in this paper we call them dissipative photovoltaic (DPV) solitons. It should be pointed out that the DPV soliton is a result of a double balance, i.e. diffraction is balanced by nonlinearity and loss is balanced by gain, which results in the DPV soliton having a fixed amplitude and width for the given dissipative system. Different from those of the previous photovoltaic solitons[14−20] which were investigated in detail by the predecessors, they should belong in the Hamiltonian system because of no energy exchanging or neglecting the loss and gain.

Because deflection is a very important subject for the study on spatial solitons in a Hamiltonian sys-

*Project supported by the National Natural Science Foundation of China (Grant Nos 10574051 and 10174025).
†E-mail: sxliu@people.com.cn
‡Corresponding author. E-mail: jsliu4508@vip.sina.com

tem, it has been extensively investigated theoretically and experimentally.[7,25−30] So far, the deflection of DPV solitons has not yet been studied in dissipative systems. However, the bending maybe plays a role in the process of DPV soliton formation since such a bending could slightly change the propagation direction of the solitary wave, thus maybe affect the coupling process between pump beam and signal beam. The experimental results in Ref.[25] demonstrate that the deflection angle is less than 0.1 degree for solitons in a Hamiltonian system, which seemingly means that the effect of bending on DPV solitons formation is too weak to be considered. The angle between pump beam and signal beam for DPV solitons was suggested to be 4 degrees,[23] so it is still necessary to study the bending property of DPV solitons. Such a study has significance not only for guiding a possible experiment of DPV solitons, but also for enriching the knowledge of spatial solitons on the properties of bending process from Hamiltonian systems to dissipative systems.

In this paper, the deflection of DPV solitons has been investigated by taking the diffusion effect into account. Firstly, by solving the CWE and the SSE using numerical technique, separately, we have testified and demonstrated that it is appropriate and valid in practice to replace CWE by SSE, i.e. under the small-signal condition, we can replace the CWE with the SSE to survey the dynamical evolution and the deflection of DPV solitons. Secondly, we have solved the SSE numerically under the small-signal condition. The numerical results reveal that the centre of the optical beam moves along a parabolic trajectory. Lastly, based on the SSE, the deflection characteristics have been analysed with a perturbational procedure, and our analyses indicate that the beam centre shifts quadratically, while the angle between the central wave-vector and propagation axis varies linearly with the propagation distance. These results gained by the perturbational model are in good agreement with those obtained by the numerical technique.

2. Nonlinear wave equation

The schematic configuration is shown in Fig.1 (also see Ref.[23]). The dissipative crystal is assumed here to be a doped KNSNB (such as Cu:KNSBN[16]) oriented along the x-axis. A one-dimensional signal beam is extraordinarily polarized, confined in the x-direction, whereas it extends in the y-direction. A strong pump beam has a uniform spatial distribution in both transverse dimensions, and it is a linearly polarized light and its polarized direction makes an angle φ with the x-axis. The signal and pump beams are made to propagate in the crystal, and the wave vector of each beam makes a small angle (θ) with the z-axis. The two coherent beams are coupled with each other by TWM and then the signal beam obtains a gain from the pump beam.[31] Under the configuration above and by using the method similar to that in Ref.[23], the space-charge field $E_{\rm sc}$ in the open-circuit dissipative PV crystal can be expressed as[7,16,23] $E_{\rm sc} = (I_{\rm b}E_{\rm eq} - I_{\rm s}E_{\rm ph})/(I_{\rm s} + I_{\rm b}) - k_{\rm B}T/[e(I_{\rm s} + I_{\rm p})]\partial I_{\rm s}/\partial x$, where $E_{\rm eq} = -\kappa E_{\rm ph}$, $\kappa = K_{\rm p}^{p}/K_{\rm p}^{e}$, $K_{\rm p}^{p}$ and $K_{\rm p}^{e}$ are the PV coefficients of the pump and signal beams, respectively, $E_{\rm ph}$ is the photovoltaic field constant of the PV crystal for the signal beam,[14−16] $k_{\rm B}$ is Boltzmann's constant, T is the absolute temperature, e is the electron charge, $I_{\rm s} = I_{\rm s}(x, z)$ is the signal beam intensity and $I_{\rm b}$ is the background light intensity. For the system considered in this paper, we have $I_{\rm b} = I_{\rm p} + I_{\rm d}$, where $I_{\rm p}$ is the pump beam intensity and $I_{\rm d}$ is the dark irradiance intensity. When $I_{\rm d} \ll I_{\rm p}$, we can develop a space-charge field with the diffusion term as follows:

$$E_{\rm sc} = -\frac{\kappa I_{\rm p} + I_{\rm s}}{I_{\rm p} + I_{\rm s}} E_{\rm ph} - \frac{k_{\rm B}T}{e}\frac{1}{I_{\rm s} + I_{\rm p}}\frac{\partial I_{\rm s}}{\partial x}. \qquad (1)$$

Then the effective refractive index is obtained as[23,32]

$$r_{\rm eff} = [\bar{n}^3 r_{33}\cos\theta\cos(\theta/2) + \bar{n} r_{42}\sin\theta\sin(\theta/2)]\cos\varphi,$$

where $\bar{n} = n_{\rm e}/n_0$, $n_{\rm e}$ is the unperturbed extraordinary refractive index, n_0 is the ordinary index of refraction, r_{33} and r_{42} are the electro-optic coefficients.

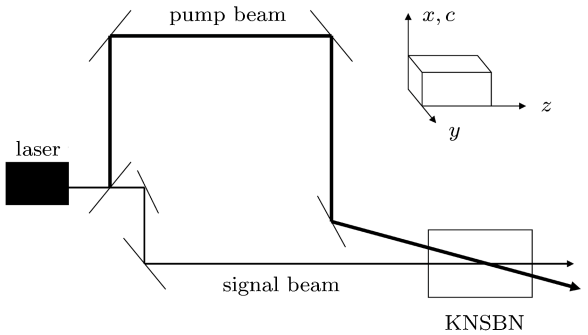


Fig.1. The schematic of a DPV in an open-circuit PV crystal, where the signal and pump beams are coupled with each other by TWM. c denotes the c-axis of the crystal.

Considering the variation of the envelope in the x-direction, in a slowly varying approximation, we find that $\phi_{\rm s}$ and $\phi_{\rm p}$ satisfy the paraxial coupled-wave equation,

$$\frac{1}{2k}\frac{\partial^2\phi_{\rm s}}{\partial x^2}+{\rm i}\cos\theta\frac{\partial\phi_{\rm s}}{\partial z}+k_0\frac{n_{\rm e}^3}{2}r_{33}\Big(E_{\rm ph}\frac{I_{\rm s}+\kappa I_{\rm p}}{I_{\rm s}+I_{\rm p}}+\frac{k_{\rm B}T}{e}\frac{1}{I_{\rm s}+I_{\rm p}}\frac{\partial I_{\rm s}}{\partial x}\Big)\phi_{\rm s}+\Big(\Gamma_0-\frac{\rm i}{2}\Gamma\Big)\frac{I_{\rm p}}{I_{\rm s}+I_{\rm p}}\phi_{\rm s}+{\rm i}\frac{1}{2}\vartheta_0\phi_{\rm s}=0,$$

$$\frac{1}{2k}\frac{\partial^2\phi_{\rm p}}{\partial x^2}+{\rm i}\cos\theta\frac{\partial\phi_{\rm p}}{\partial z}+k_0\frac{n_{\rm e}^3}{2}r_{33}\Big(E_{\rm ph}\frac{I_{\rm s}+\kappa I_{\rm p}}{I+I_{\rm p}}+\frac{k_{\rm B}T}{e}\frac{1}{I_{\rm s}+I_{\rm p}}\frac{\partial I_{\rm s}}{\partial x}\Big)\phi_{\rm p}+\Big(\Gamma_0+\frac{\rm i}{2}\Gamma\Big)\frac{I_{\rm s}}{I_{\rm s}+I_{\rm p}}\phi_{\rm p}+{\rm i}\frac{1}{2}\vartheta_0\phi_{\rm p}=0, \quad (2)$$

where $k=n_{\rm e}k_0$ is the wave vector, $k_0=2\pi/\lambda_0$, λ_0 is the free-space wavelength of the light wave, Γ and Γ_0 are the intensity and phase coupling coefficients of the TWM process, respectively, ϑ_0 is the absorption coefficient of the dissipative crystal. One can adopt the dimensionless form $\xi=z/(z_0\cos\theta)$, $s=x/x_0$, $z_0=kx_0^2$, $g_0=z_0\Gamma_0$, $g=z_0\Gamma/2$, $\vartheta=z_0\vartheta_0/2$, $U_{\rm s}=I_0^{-1/2}\phi_{\rm s}$ and $U_{\rm p}=I_0^{-1/2}\phi_{\rm p}$, where x_0 is an arbitrary spatial width and I_0 is an arbitrary intensity. Thus Eq.(2) can be expressed in terms of $U_{\rm s}$ and $U_{\rm p}$ as

$${\rm i}\frac{\partial U_{\rm s}}{\partial\xi}+\frac{1}{2}\frac{\partial^2U_{\rm s}}{\partial s^2}+[\alpha(|U_{\rm s}|^2+\kappa|U_{\rm p}|^2)+\gamma(|U_{\rm s}|^2)_{\rm ps}]\frac{U_{\rm s}}{|U_{\rm p}|^2+|U_{\rm s}|^2}+(g_0-{\rm i}g)\frac{|U_{\rm p}|^2}{|U_{\rm p}|^2+|U_{\rm s}|^2}U_{\rm s}+{\rm i}\vartheta U_{\rm s}=0,$$

$${\rm i}\frac{\partial U_{\rm p}}{\partial\xi}+\frac{1}{2}\frac{\partial^2U_{\rm p}}{\partial s^2}+[\alpha(|U_{\rm s}|^2+\kappa|U_{\rm p}|^2)+\gamma(|U_{\rm s}|^2)_{\rm ps}]\frac{U_{\rm p}}{|U_{\rm p}|^2+|U_{\rm s}|^2}+(g_0+{\rm i}g)\frac{|U_{\rm s}|^2}{|U_{\rm p}|^2+|U_{\rm s}|^2}U_{\rm p}+{\rm i}\vartheta U_{\rm p}=0, \quad (3)$$

where $\alpha=\chi r_{33}E_{\rm ph}$, $\gamma=\chi r_{33}\tau$, $\chi=(k_0x_0)^2(n_{\rm e}^4/2)$, $\tau=k_{\rm B}T/(ex_0)$, $(|U_{\rm s}|^2)_{\rm ps}=\partial(|U_{\rm s}|^2)/\partial s$. Equation (3) is the very coupled-wave equation (CWE) mentioned above.

Owing to $\Gamma_0+{\rm i}\Gamma/2={\rm i}\delta\tilde{E}E_{\rm sa}/(\tilde{E}+E_{\rm sa})$, where $\delta=n_{\rm e}^3r_{\rm eff}k_0/2$, $\tilde{E}=E_{\rm d}-{\rm i}E_{\rm eq}$, $E_{\rm d}=4\pi k_{\rm B}T\sin\theta/(\lambda_0e)$ is the diffusion field, $E_{\rm sa}=eN_{\rm A}\lambda_0/(4\pi\varepsilon_{\rm r}\varepsilon_0\sin\theta)$ is the saturation field, $E_{\rm ds}=E_{\rm d}+E_{\rm sa}$, $N_{\rm A}$ is the acceptor density, ε_0 is the permittivity of vacuum, $\varepsilon_{\rm r}$ is the relative static dielectric constant, we can obtain the expressions for g and g_0 as, respectively,

$$g=\chi r_{\rm eff}\frac{E_{\rm sa}(E_{\rm eq}^2+E_{\rm d}E_{\rm ds})}{E_{\rm ds}^2+E_{\rm eq}^2},\quad g_0=\chi r_{\rm eff}\frac{E_{\rm eq}E_{\rm sa}^2}{E_{\rm ds}^2+E_{\rm eq}^2}.$$

Under the undepleted pump approximation and by ignoring the effect of self-focusing nonlinearity on the pump beam (also called the small-signal condition), we can take $U_{\rm p}(x,z)$ as a constant.[23] As a result, the CWE (3) degenerates into

$${\rm i}\frac{\partial U_{\rm s}}{\partial\xi}+\frac{1}{2}\frac{\partial^2U_{\rm s}}{\partial s^2}-[Q-\gamma(|U_{\rm s}|^2)_{\rm ps}+{\rm i}G]U_{\rm s}+[P-\gamma(|U_{\rm s}|^2)_{\rm ps}+{\rm i}g]|U_{\rm s}|^2U_{\rm s}=0, \quad (4)$$

where $Q=-\kappa\alpha-g_0$, $G=g-\vartheta$ and $P=\alpha(1-\kappa)-g_0$. Equation (4) is the very small-signal equation (SSE) mentioned above. When $\gamma=0$, the bright soliton solution of SSE (4) reads[23]

$$U_{\rm s}(s,\xi)=F{\rm sech}(Bs)\times\exp\{{\rm i}b\ln[{\rm sech}(Bs)]\}\exp(-{\rm i}\nu\xi), \quad (5)$$

where $F=[3G/(2g)]^{1/2}$ is the amplitude, $B=(G/b)^{1/2}$ is the parameter related to width, $b=[-3P+(9P^2+8g^2)^{1/2}]/(2g)$ is the chirp parameter, $\nu=(b^2-1)G/(2b)+Q$ is the parameter to represent the nonlinear shift of the propagation constant.

3. The equivalence between the small-signal equation and the coupled-wave equation under small-signal condition

When the diffusion effect is neglected, the analytical solitary solutions can be obtained from Eq. (4). Taking the bright soliton solution, i.e. Eq. (5), as an input beam, the dynamical evolution of this input beam in a dissipative system can be studied by numerically solving the SSE (4) and the CWE (3), separately. For the latter, a Super-Gauss beam is needed as an input pump beam, i.e. $U_{\rm p}(s,\xi=0)=I_{\rm p}^{1/2}\exp[-(s/b_0)^4]$, where, $I_{\rm p}$ is the peak intensity normalized by I_0, b_0 is a parameter corresponding to the width of the beam. It will be demonstrated that, under the small-signal condition, that is, the signal beam is much weaker than the pump beam, the behaviours of the dynamical evolution of the input signal beam revealed by the two (SSE and CWE) equations are almost the same, including the process of deflection

by considering the diffusion. This allows us to use SSE (4), instead of CWE (3), to investigate the deflection of DPV solitons via not only a numerical method in Subsection 4.1, but also a perturbation procedure in Subsection 4.2.

For this dissipative system, the values of those parameters in the above equations that will be used in the following numerical simulations are taken as $n_e = 2.27$, $n_0 = 2.35$, $\varepsilon_r = 500$, $r_{33} = 200$ pm/V and $r_{42} = 820$ pm/V for a KNSBN crystal with $N_A = 1.2 \times 10^{16}$ cm^{-3}, $\vartheta_0 = 0.54$ cm^{-1} for $\lambda_0 = 0.5$ μm at $T = 300$ K, the other variables are $\theta = 2°$, $\varphi = 87°$, $E_{ph} = 2030$ V/cm,[23] the arbitrary scale $x_0 = 25$ μm, as well as $\kappa = 0.5$.[16]

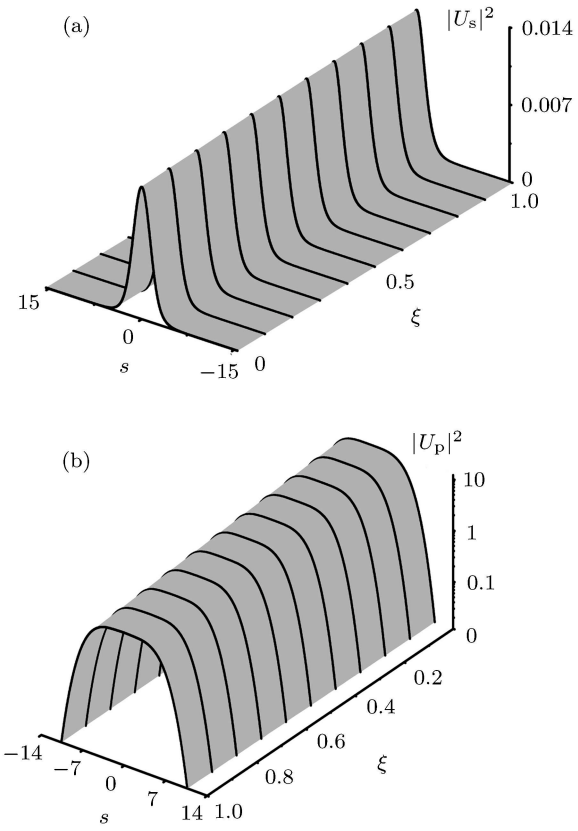


Fig.2. (a) Simultaneous evolution of a bright DPV soliton (intensity profile) based on the CWE by neglecting the diffusion effect. Here, the adopted system parameters are $\theta = 2°$ $\varphi = 87°$, $\lambda = 0.5$ μm, $T = 300$ K, $E_{ph} = 2030$ V/cm, $\alpha = 53.1985$, $\gamma = 0$, $\vartheta_0 = 0.54$ cm^{-1} and $\kappa = 0.5$. Solution parameters are $F = 0.113211$, $B = 0.595924$, $b = 0.0116818$ and $\nu = -25.6699$. (b) Simultaneous evolution of the pump beam, where $U_p(s, \xi = 0) = I_p^{1/2}\exp[-(s/b_0)^4]$, $b_0 = 12$ μm, the dimensionless $I_p = 12$.

With the set of values above and letting $\gamma = 0$, the intensity evolutions of the bright DPV soliton in the dissipative crystal are obtained and shown in Fig.2(a) and Fig.3 by solving numerically CWE (3) and SSE (4), separately. They have revealed that, under the small-signal condition, the intensity profile evolution obtained by solving the CWE is in good agreement with those obtained by using the SSE. At the same time, under the set of the system parameter values above and by taking the diffusion effect into account, we have again obtained and compared the results based on both equations. The intensity evolutions of the bright DPV soliton are obtained and shown in Fig.4(a) and Fig.4(b). In addition, the results of spatial shift (Δs) due to the diffusion effect are illustrated in Fig.4(c). The numerical results reveal that the small-signal equation is also valid and feasible under the small-signal condition when $\gamma \neq 0$, i.e. for describing the deflection of DPV solitons, the SSE (4) is the equivalence of the CWE (3) under small-signal condition.

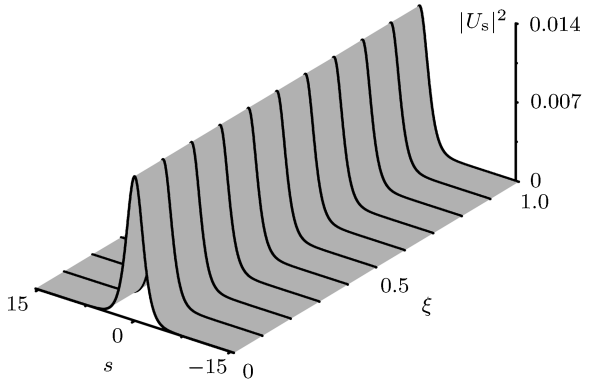


Fig.3. Simultaneous evolution of a bright DPV soliton (intensity profile) based on the SSE by neglecting the diffusion effect. Here the adopted system parameters and solution parameters are the same as those in Fig.2(a).

Without losing the universality, we have repeated the numerical simulation of CWE (3) and SSE (4) in a very broad range of system parameters. The numerical simulation results show that it is feasible and valid to replace the CWE with the SSE under small-signal condition.

In virtue of the analyses above, we have verified the feasibility and validity of the small-signal equation. It provides us a convenient way to investigate the deflection of DPV solitons. That is, CWE (3) can be replaced by SSE (4) to investigate the deflection of DPV solitons under small-signal condition.

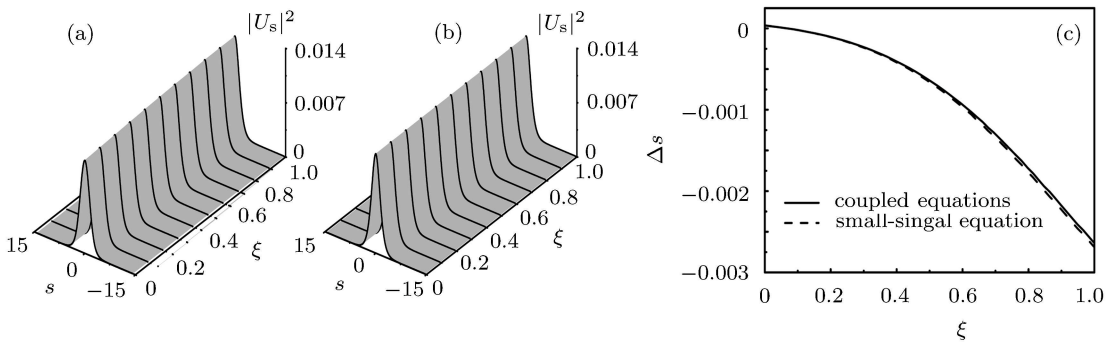


Fig.4. (a) Simultaneous evolution of a bright DPV soliton (intensity profile) by considering the diffusion effect, based on the CWE; (b) Simultaneous evolution, based on the SSE; (c) Evolution of the normalized spatial shift Δs, based on the CWE (the solid curve) and the SSE (the dashed curve). Here, the adopted system parameters and solution parameters are the same as those in Fig.2(a) excepting $\gamma = 0.2710$.

4. Deflection of bright DPV solitons

4.1. Numerical simulation results

Under the small-signal condition, the deflection of DPV solitons is investigated via numerically solving SSE (4) for a series of combinations of system parameters. The appropriate parameters have been selected in order to support and form a stable DPV soliton. Here we have computed some groups of parameter values in Tables 1–3, separately. Meanwhile, the deflections of DPV solitons have been gained via numerical method, the normalized spatial shifts (Δs) are shown in Figs.6–8. These results indicate that the bright DPV soliton moves on an approximately parabolic trajectory, i.e. it evolves approximately along a parabolic trajectory during propagation, which is similar to the behaviour of solitons in a Hamiltonian system. But it should be noticed that the deflection degrees of DPV solitons are very small under the small-signal condition. Regarding the actual propagating distance $z = 1$ cm of the solitary beam in the dissipative system as a standard, the corresponding deflection angle (denoted by ψ) of DPV soliton is also attached to the parameters in Tables 1–3. The definition of deflection angle is illustrated in Fig.5.

Table 1. The variable parameters used in Fig.6 and deflection angles.

θ	φ	$E_{\rm ph}$	α	F	B	b	ν	$\psi/(^\circ)$
3	87	1230	32.2336	0.11682	0.477821	0.0193579	−15.6207	1.06×10^{-4}
2	87	2030	53.1985	0.113211	0.595924	0.0116818	−25.6699	1.24×10^{-4}
2	88	3020	79.1426	0.11347	0.72322	0.00796811	−38.7819	1.51×10^{-4}
5	89	4760	124.741	0.0789222	0.624894	0.00514021	−62.2450	0.64×10^{-4}

Table 2. The variable parameters used in Fig.7 and deflection angles.

T	$E_{\rm ph}$	α	γ	F	B	b	ν	$\psi/(^\circ)$
280	2100	55.0329	0.252928	0.105319	0.563894	0.011278	-26.5269	0.95×10^{-4}
300	2030	53.1985	0.270994	0.113211	0.595924	0.0116818	-25.6699	1.24×10^{-4}
320	1950	51.102	0.28906	0.101342	0.522802	0.0121415	-24.6273	0.93×10^{-4}

Table 3. The variable parameters used in Fig.8 and deflection angles.

ϑ_0	$E_{\rm ph}$	α	F	B	b	ν	$\psi/(^\circ)$
0.54	2030	53.1985	0.113211	0.595924	0.0116818	-25.6699	1.2389×10^{-4}
0.65	2471	64.7554	0.112984	0.655927	0.0115596	-31.2690	1.3582×10^{-4}
0.72	2721	71.3069	0.111697	0.680318	0.0116309	−34.4437	1.3769×10^{-4}

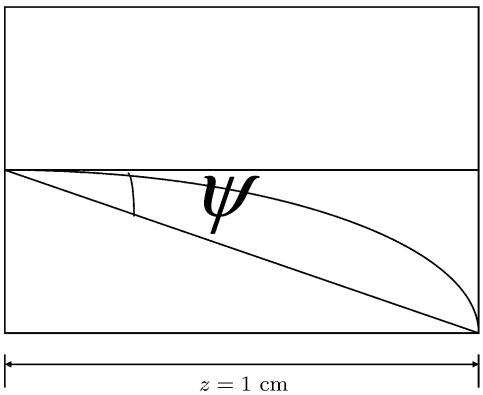


Fig.5. The schematic of the deflection angle, when a DPV soliton propagates the distance $z = 1$ cm in an open-circuit dissipative PV crystal.

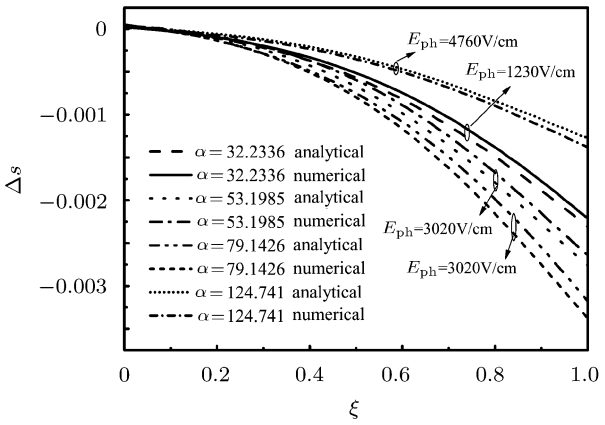


Fig.6. The normalized spatial shift Δs versus ξ, where the values of the system parameters are given as $x_0 = 25$ μm, $\lambda_0 = 0.5$ μm, $T = 300$ K, $\vartheta_0 = 0.54$ cm^{-1} and $\gamma = 0.270994$, and the other parameters and solution parameters are indicated in Table 1.

From Fig.6, it is easily found that the deflection of DPV soliton is related to α, but it is not affirmed that a larger deflection degree is corresponding to a higher value of α. Now that the diffusion item γ is a function of temperature T, i.e. the value of γ varies with T, the relation between the deflection of DPV solitons and γ is shown in Fig.7, from which one can find that the bending degree does not become larger with the γ being higher, but it lies on the parameters of the dissipative system. Moveover, it is seen from Fig.8 that the deflection degree of DPV soliton is not very sensitive to the absorption coefficient ϑ_0. Based on the bending angle ψ in Tables 1–3, it is convinced that the deflection degree of DPV soliton is slight under the small-signal condition. From Figs.6–8, we can also assure that the deflection degree of DPV soliton is determined by the system parameters, that is to say, the DPV soliton has the fixed deflection for the fixed system parameters, which is the same as the behaviour of the RPV solitons[23] that have the fixed amplitude and width for the fixed values of system parameters. That is the very reason why it is called 'rigid' soliton in the dissipative system. It should be emphasized that we discuss the deflection of the DPV soliton on condition that it can exist and propagate stably in the dissipative system, because the parameters of DPV soliton vary as the system parameters change.

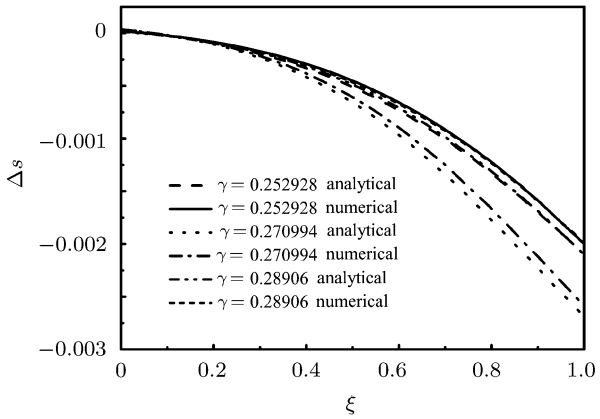


Fig.7. The normalized spatial shift Δs versus ξ, where the values of the system parameters are given as $x_0 = 25$ μm, $\lambda_0 = 0.5$ μm, $\theta = 2°$, $\varphi = 87°$, $E_{\rm ph} = 2030$ V/cm and $\vartheta_0 = 0.54$ cm^{-1}, and the other system parameters and solution parameters are shown in Table 2.

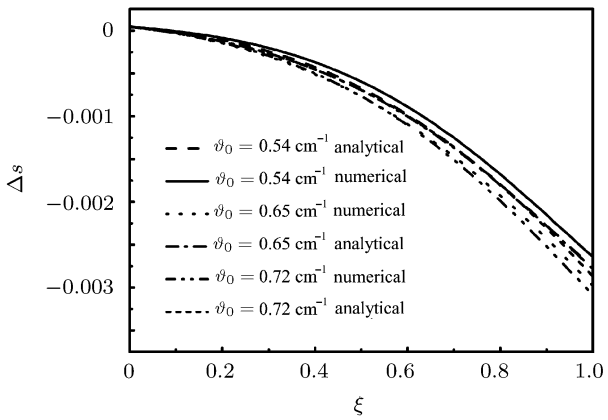


Fig.8. The normalized spatial shift Δs versus ξ, where the values of the system parameters are given as $\theta = 2°$, $\varphi = 87°$, $x_0 = 25$ μm, $\lambda_0 = 0.5$ μm, $T = 300$ K and $\gamma = 0.270994$, and the other system parameters and solution parameters can be found in Table 3.

4.2. Perturbational procedure and results

Here, the deflection effect of the DPV soliton will be further investigated theoretically, i.e. through solving SSE (4) by the perturbational procedure.[7,28]

Keeping in mind that the beam evolution under the action of diffusion is approximately adiabatic,[28] we start by making the following ansatz for the solution of SSE (4):

$$U_{\rm s}(s,\xi) = P^{-1/2}V[s+\mu(\xi)]\exp\{-{\rm i}[Q\xi+\omega(\xi) \times (s+\mu(\xi))+\sigma(\xi)]\}, \quad (6)$$

where $U_{\rm s}(s,\xi) = P^{-1/2}V(s,\xi)\exp(-{\rm i}Q\xi)$ is the steady-state bright DPV soliton of SSE (4) with $\gamma = 0$. In Eq.(6) $\mu(\xi)$ represents a shift in the position of the beam centre, $\omega(\xi)$ is related to the angle between the central wave vector of this beam and the propagation axis ξ, $\sigma(\xi)$ is a phase factor that varies during propagation. The equations of motion for these real variables are obtained by substituting Eq.(6) into two complex conservation laws of SSE (4). These are established by multiplying SSE (4) with $U_{\rm s}^*$ and $(U_{\rm s})_{\rm s}^*$ and integrating from $-\infty$ to $+\infty$ over the coordinate s. The results are given as

$$\frac{{\rm d}\mu(\xi)}{{\rm d}\xi} = \omega(\xi), \quad (7)$$

$$\frac{{\rm d}\sigma(\xi)}{{\rm d}\xi} = -\frac{\omega^2(\xi)}{2}, \quad (8)$$

$$\frac{{\rm d}\omega(\xi)}{{\rm d}\xi} = -4\gamma K_P, \quad (9)$$

where the dimensionless K_P is given by

$$\begin{aligned} K_P &= \left| \int_{-\infty}^{\infty} (b-{\rm i})^2 B^2 F^2 \sinh^2(Bs)\,{\rm sech}(Bs)^{4+2{\rm i}b}[F^2{\rm sech}(Bs)^{2+2{\rm i}b}-1]{\rm d}s \right| \\ &= \left| \frac{1}{16}(b-{\rm i})BF^2\Big\{ \frac{12+4{\rm i}b}{b-2{\rm i}} - 4{\rm i}F^2 + \frac{2\sqrt{\pi}(b-{\rm i})\Gamma(3+{\rm i}b)}{\Gamma(7/2+{\rm i}b)} \right. \\ &\quad + (b-{\rm i}){\rm e}^{b\pi}[4^{3+{\rm i}b}B_{-1}(5+{\rm i}b,-5-2{\rm i}b) + 2^{8+4{\rm i}b}{\rm e}^{b\pi}F^2 B_{-1}(4+2{\rm i}b,-5-4{\rm i}b)] \\ &\quad \left. + \frac{\sqrt{\pi}b\Gamma(5+{\rm i}b)}{(b-2{\rm i})^2\Gamma(7/2+{\rm i}b)} - \frac{8\sqrt{\pi}(b-{\rm i})F^2\Gamma(3+2{\rm i}b)}{\Gamma(7/2+2{\rm i}b)} - \frac{2\sqrt{\pi}{\rm i}F^2\Gamma(4+2{\rm i}b)}{\Gamma(7/2+2{\rm i}b)} - \frac{4^{3+{\rm i}b}\Gamma(2+{\rm i}b)\Gamma 5+{\rm i}b}{(b-2{\rm i})\Gamma(6+2{\rm i}b)} \Big\} \right|. \quad (10) \end{aligned}$$

Here $B_z(a,b)$ is the incomplete *Beta* function and $\Gamma(z)$ is the *Euler Gamma* function, viz. $B_z(a,b) = \int_0^z t^{a-1}(1-t)^{b-1}{\rm d}t$ and $\Gamma(z) = \int_0^{+\infty} t^{z-1}{\rm e}^{-t}{\rm d}t$, so the term of K_P is a constant.

Integrating Eqs.(7)–(9) yields the equations of motion

$$\omega(\xi) = -4\gamma K_P\xi, \quad (11)$$

$$\mu(\xi) = -2\gamma K_P\xi^2, \quad (12)$$

$$\sigma(\xi) = -8\gamma^2 K_P^2\xi^3/3. \quad (13)$$

Equations (11)–(13) demonstrate that, in the absence of diffusion, i.e. $\gamma = 0$, the variables $\omega = \mu = \sigma = 0$. However, by taking diffusion effect into account, Eq.(12) shows that the beam centre follows a parabolic trajectory, whereas Eq.(11) implies that the central spatial frequency component shifts linearly with the propagation distance, which is similar to the behaviour of Hamiltonian solitons. Also, it is easily found that the beam has suffered a lateral displacement with a distance given by

$$x_{\rm d} = 2\gamma K_P z^2/(k_0^2 n_{\rm e}^2\cos^2\theta x_0^3) \quad \text{or}$$

$$x_{\rm d} = 2r_{33}(k_{\rm B}T/2e)K_P z^2/(x_0^2\cos^2\theta), \quad (14)$$

where z is the actual propagation distance. Moreover, the angular deflection, i.e. the angle between the central wave vector of this soliton beam and the z-axis can also be evaluated from Eq.(11) and is given by

$$\theta_{\rm d} = 4\gamma K_P z/(k_0^2 n_{\rm e}^2\cos^2\theta x_0^3) \quad \text{or}$$

$$\theta_{\rm d} = 4r_{33}(k_{\rm B}T/2e)K_P z/(x_0^2\cos^2\theta). \quad (15)$$

It is important to know whether $\omega(\xi)$, $\mu(\xi)$ and $\sigma(\xi)$, or $x_{\rm d}$ and $\theta_{\rm d}$ are also related to α implicated in the term of K_P, which is associated with the photovoltaic process. It is revealed that K_P is together determined by values of F, B and b from Eq.(10), in other words, it is not assured that K_P is proportionable to α. Thus the deflection degree is not larger when the value of α is higher due to Eq.(12), which agrees with the numerical result (Fig.6).

Some groups of the system parameters and solution parameters have been illustrated in Tables 1–3. Also, the normalized spatial shifts ($\Delta s = \mu$) predicted by an analytical model have been compared with those

obtained numerically in Figs.6–8, respectively. As one can see, the results from both approaches are consistent with each other on the whole. There is a small difference between the numerical results and those obtained from the analytical model: the numerical results are less than the analytical ones, which can be attributed to the fact that the evolution of bright DPV solitons under the action of diffusion is not entirely adiabatic. In addition, Figs.6–8 present that the deflection degree of DPV solitons is small and determined by dissipative system parameters under the small-signal condition, which is very different from the behaviour of solitons in a Hamiltonian system.

5. Conclusion

In conclusion, by considering the diffusion effect, the deflection of bright DPV solitons has been discussed by both numerical simulation and perturbational procedure. By using numerical technique, we have found that the deflection of the signal beam is approximately parabolic, which is further studied using a perturbational model. As one can see, the results from two approaches are in good agreement with each other. We have found that the centre of the solitary beam moves on a parabolic trajectory, whereas its central spatial frequency component shifts linearly with the propagation distance. The deflection property of DPV solitons in a dissipative system is similar to that of solitons in a Hamiltonian system. The deflection degree is very weak under the small-signal condition, and it is determined by the parameters of the dissipative system. Because DPV solitons are based on the process of TWM between pump beam and signal beam, the deflection of the signal beam may affect the soliton formation of the signal beam in possible experiments. Our results demonstrate that the bending angles are very small. The slight bending does not influence the formation of the DPV soliton in a dissipative system, which gives a guarantee that a stable DPV soliton can exist and form in a dissipative crystal via two-wave mixing, the DPV soliton is little influenced or totally destroyed by the diffusion effect in theory and experiment. Therefore, the most essential prediction from this study for possible experiments may be that the deflection of the beams is a factor that could be ignored in the process of DPV soliton formation.

References

[1] Segev M, Crosignani B, Yariv A and Fischer B 1992 *Phys. Rev. Lett.* **68** 923
[2] Duree G C, Shultz J L, Salamo G J, Segev M, Yariv A, Sharp E J and Neurgaonkar R R 1993 *Phys. Rev. Lett.* **71** 533
[3] Geisler A, Homann F and Schmidt H J 2004 *Opt. Commun.* **238** 351
[4] DelRe E, D'Ercole A and Palange E 2005 *Phys. Rev.* E **71** 036610
[5] Segev M, Valley G C, Crosignani B Porto, P D and Yariv A 1994 *Phys. Rev. Lett.* **73** 3211
[6] Christodoulides D N and Carvalho M I 1995 *J. Opt. Soc. Am.* B **12** 1628
[7] Liu J S and Lu K Q 1999 *J. Opt. Soc. Am.* B **16** 550
[8] Andrade-Lucio J A, Iturbe-Castillo M D, Marquez-Aguilar P A and Ramos-Garcia R 1998 *Opt. Quantum Electron.* **30** 829
[9] Guo Q and Xu C B 2004 *Acta Phys. Sin.* **53** 3025 (in Chinese)
[10] Guo Q, Zhang X P, Hu W and Shou Q 2006 *Acta Phys. Sin.* **55** 1832 (in Chinese)
[11] DelRe E, Ciattoni A and Palange E 2006 *Phys. Rev.* E **73** 017601
[12] Taya M, Bashaw M C, Fejer M M, Segev M and Valley G C 1996 *Opt. Lett.* **21** 943
[13] Chen Z G, Segev M, Wilson D W, Muller R E and Maker P D 1997 *Phys. Rev. Lett.* **78** 2948
[14] Valley G C, Segev M, Crosignani B, Yariv A, Fejer M M and Bashaw M C 1994 *Phys. Rev.* A **50** R4457
[15] Segev M, Valley G C, Bashaw M, Taya M and Fejer M M 1997 *J. Opt. Soc. Am.* B **14** 1772
[16] She W L and Lee W K 1999 *Phys. Rev. Lett.* **83** 3182
[17] Taya M, Bashaw M C, Fejer M M, Segev M and Valley G C 1995 *Phys. Rev.* A **52** 3095
[18] Lu Y, Liu S M, Guo R, Yang L S, Huang C F and Wang D Y 2003 *Acta Phys. Sin.* **52** 3075 (in Chinese)
[19] Hou C F, Pei Y B, Zhou Z X and Sun X D 2005 *Chin. Phys.* **14** 349
[20] Ouynag S G and She W L 2004 *Acta Phys. Sin.* **53** 3042 (in Chinese)
[21] Cohen O, Carmon T, Segev M and Odoulov S 2002 *Opt. Lett.* **27** 2031
[22] Liu J S and Du Z M 2005 *Acta Phys. Sin.* **54** 2739 (in Chinese)
[23] Liu J S 2003 *Phys. Rev.* E **68** 026607
[24] Królikowski W, Luther-Davies B and Denz C 2003 *IEEE J. Quantum Electron.* **39** 3
[25] Petter J, Weilnau C, Denz C, Stepken A and Kaiser F 1999 *Opt. Commun.* **170** 291
[26] Shih M F, Leach P, Sergev M, Garret M H, Gsalamo and Valley G C 1995 *Opt. Lett.* **21** 324
[27] Singh S R and Christodoulides D N 1995 *Opt. Commun.* **118** 569
[28] Carvalho M I, Singh S R and Christodoulides D N 1995 *Opt. Commun.* **120** 311
[29] Chauvet M, Coda V, Maillotte H, Fazio E and Salamo G 2005 *Opt. Lett.* **30** 1977
[30] Liu J S and Hao Z H 2003 *Chin. Phys.* **12** 1124
[31] Yeh P 1989 *IEEE J. Quantum Electron.* **25** 484
[32] Oda I, Otani Y, Liu L and Yoshizawa T 1998 *Opt. Commun.* **148** 95